Chaotic motors

C. Laroche, R. Labbé, F. Pétrélis, and S. Fauve

Chaotic motors

C. Laroche
Laboratoire de Physique Statistique, Ecole Normale Supérieure, Université P. et M. Curie, Université Paris Diderot, CNRS, 24 rue Lhomond, F-75005 Paris, France

R. Labbé
Laboratorio de Turbulencia and GCTE, Departamento de Física, Facultad de Ciencia, Universidad de Santiago de Chile, USACH, Casilla 307, Correo 2, 9170022, Santiago, Chile

F. Pétrélis and S. Fauve
Laboratoire de Physique Statistique, Ecole Normale Supérieure, Université P. et M. Curie, Université Paris Diderot, CNRS, 24 rue Lhomond, F-75005 Paris, France

(Received 2 August 2011; accepted 8 November 2011)

We show that electric motors and dynamos can be used to illustrate most elementary instabilities or bifurcations discussed in courses on nonlinear oscillators and dynamical systems. These examples are easier to understand and display a richer behavior than the ones commonly used from mechanics, electronics, hydrodynamics, lasers, chemical reactions, and population dynamics. In particular, an electric motor driven by a dynamo can display stationary, Hopf, and codimension-two bifurcations by tuning the driving speed of the dynamo and the electric current in the stator of the electric motor. When the dynamo is driven at constant torque instead of constant rotation rate, chaotic reversals of the generated current and of the angular rotation of the motor are observed. Simple deterministic models are presented which capture the observed dynamical regimes.

[DOI: 10.1119/1.3664605]

I. INTRODUCTION

Many textbooks on instabilities and bifurcation phenomena have been published since the early 1980s when chaos and more generally nonlinear physics became fashionable. Most of these textbooks introduce these subjects from the point of view of applied mathematics,[1–4] and primarily discuss the solutions of nonlinear differential equations. Some of them put more emphasis on physical and engineering examples or on analogies between instabilities and phase transitions.[5,6] Examples of instabilities in mechanical or electromechanical systems, electronics, feedback loops, can be also found in the earlier literature.[7] However, most simple examples concern stationary instabilities. It is more difficult to find simple illustrations of an oscillatory instability (a Hopf bifurcation) or a codimension-two bifurcation, that is, a situation in which two different instabilities are in competition. Electronic oscillators provide good examples of oscillatory instabilities,[5,7] but require some knowledge of electronics which is becoming less common among physics students. Oscillatory chemical reactions are sometimes considered,[8] but they are studied using ad hoc models and quantitative experiments are difficult. Hydrodynamic instabilities can display oscillatory behavior,[9] but their description involves lengthy calculations and cannot be used as simple illustrative examples.

The generation of electricity from mechanical work using a dynamo or the reverse process using a motor is usually analyzed by focusing on stationary regimes as achieved in the common daily applications of electromagnetic machines (see, for example, Refs. 10–14). We will show that a dynamo driving an electric motor can display both stationary and oscillatory instabilities by changing parameters. In Sec. II, we consider the simplest dynamo model, the Bullard dynamo, driving a Faraday disk used as a motor. This example requires only some elementary knowledge of electromagnetism and illustrates stationary, Hopf, and codimension-two bifurcations. It also displays chaotic regimes. However, the experimental realization of a Bullard dynamo cannot be easily achieved. We show in Sec. III that a low cost universal motor can be used to perform a simple study of the dynamo effect. The model presented in Sec. IV shows how the saturation mechanism can lead to supercritical or subcritical stationary bifurcations. In Sec. V, we show how this dynamo can be used to drive a similar motor. Depending on the electric current in the stator, this device either displays a stationary or oscillatory regime. In the latter, both the current generated by the dynamo and the angular rotation speed of the motor reverse periodically. If the dynamo is driven at constant torque instead of constant velocity, these reversals can be chaotic.

II. THE FARADAY DISK AND THE BULLARD DYNAMO

A. A stationary bifurcation illustrated by the Bullard dynamo

The generation of an electric current from mechanical work is a common process. It is straightforward to generate an electric current by rotating a conductor in an external magnetic field, but to do so requires a pre-existing current or a permanent magnet. Finding how to convert mechanical power into electricity without the aid of permanent magnetism or an externally imposed field was a great achievement by Siemens, Wheatstone, and others at the end of the nineteenth century.[15] It is not always emphasized that this transformation of mechanical work into electromagnetic energy relies on an instability mechanism, as we will discuss in the following.

We will first illustrate this process using a simple example which does not require prior knowledge of dynamos and electric motors. We consider a conducting disk of radius a in an externally applied magnetic field $\vec{B}_0$ [see Fig. 1(a)]. This arrangement is called a Faraday disk. The electromotive force $\mathcal{E}$ between the points A and P can be easily calculated from the law of induction

$$\mathcal{E} = \int_{AP} \left[(\vec{\Omega} \times \vec{r}) \times \vec{B}_0 \right] \cdot d\vec{r} = \frac{1}{2}\Omega a^2 B_0, \tag{1}$$

and generates a current $I = \mathcal{E}/R$ in the circuit of resistance R. Is it possible to use this current to generate the magnetic field $\vec{B}_0$? This question might seem strange, but leads to a typical instability problem. The answer is yes if the geometry of the circuit is such that a perturbation of the current generates a magnetic field which amplifies the current by electromagnetic induction. The simplest way to achieve self-generation of a current or a magnetic field is the Bullard dynamo displayed in Fig. 1(a). Ohm's law gives

$$L\frac{dI}{dt} + RI = \mathcal{E} = M\Omega I, \tag{2}$$

where L is the inductance of the circuit and M is the mutual inductance between the wire and the disk. From Eq. (1) it follows that $\mathcal{E}$ is proportional to Ω and I, which generates the magnetic field **B**.

By using Eq. (2), the stability analysis of the solution $I = 0$ (corresponding to $B = 0$) is straightforward. The current I and thus the magnetic field B are exponentially amplified if $\Omega > \Omega_c = R/M$. The self-generation of current depends on the sign of the rotation rate. This result is not surprising because the wire breaks the mirror symmetry with respect to any plane containing the axis of rotation. The direction of winding of the wire gives the sign of M, and thus determines the sign of Ω for self-generation.

We have obtained the condition for the onset of dynamo action. For a rotation rate greater than Ω_c, Eq. (2) implies that the current is exponentially growing. This process should stop at some stage as shown by the equation for the angular rotation rate

$$J\frac{d\Omega}{dt} = \Gamma - \lambda\Omega - MI^2, \tag{3}$$

where J is the moment of inertia of the disk, Γ is the torque driving the disk, and the mechanical friction torque is assumed to be proportional to the rotation rate (λ is constant). The last term on the right-hand side of Eq. (3) results from the Lorentz force generated by the magnetic field $\vec{B}$ acting on the current density $\vec{j}$ in the disk

$$\int \vec{r} \times (\vec{j} \times \vec{B})\, d^3r = MI^2\hat{z}, \tag{4}$$

where $\hat{z}$ is normal to the plane of the disk. This force is opposite to the motion of the disk and is proportional to I^2.

It can be easily checked that the proportionality constant in Eq. (4) is M by looking at the energy budget. We multiply Eq. (2) by I and Eq. (3) by Ω, add the results, and obtain

$$\frac{d}{dt}(J\Omega^2 + LI^2)/2 = (\Gamma - \lambda\Omega)\,\Omega - RI^2. \tag{5}$$

In a stationary regime the power of the motor is dissipated by mechanical losses and Joule heating. The two contributions proportional to ΩI^2 have to cancel to have energy conservation in the absence of dissipative mechanisms and forcing. The growth of the current is bounded by the available mechanical power. The stationary solutions of Eqs. (2) and (3) are $I = 0$ and $\Omega = \Gamma/\lambda$ if $\Gamma < \Gamma_c = \lambda R/M$. If $\Gamma > \Gamma_c$, we have $\Omega = \Omega_c$ and $I^2 = (\Gamma - \Gamma_c)/M$.

In this simple example there is a stationary bifurcation for $\Gamma = \Gamma_c$. The broken symmetry at the instability onset is the $B \to -B$ symmetry or the $I \to -I$ symmetry of Eqs. (2) and (3). Although the bifurcated branches of the solution for I for $\Gamma > \Gamma_c$ display the usual behavior, that is, the growth of I proportional to the square-root of the distance to criticality, Ω is constant in this regime because we have neglected the possible nonlinear saturation mechanisms (for example, the dependence of L or M on B) in Eq. (2). As we will discuss this behavior does not exist for realistic dynamos and electric motors.

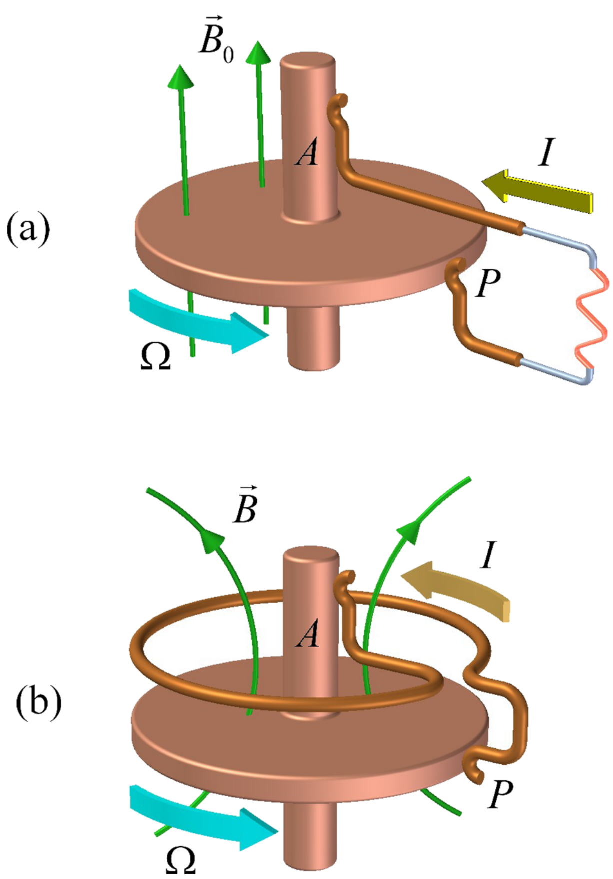

Fig. 1. (a) Sketch of the Faraday inductor. (b) Sketch of the Bullard dynamo.

B. A Bullard dynamo driving a Faraday disk: Hopf and codimension-two bifurcations

We now use the electrical current provided by the Bullard dynamo to drive a Faraday disk working as a motor (see Fig. 2). We first write the governing equations for the current I and the rotation rate Ω_2 of the dynamo. In addition to the effects described in Eq. (2), we have to take into account the back electromotive force of the Faraday disk which is equal to $-\alpha B_0 \Omega_2$ where $\alpha = a^2/2$. The Faraday disk is driven by the torque of the Lorentz force which is proportional to B_0 and I, with the constant of proportionality equal to α as can be found by using energy conservation. We obtain

$$L\frac{dI}{dt} = (M\Omega_1 - R)I - \alpha B_0 \Omega_2 \tag{6}$$

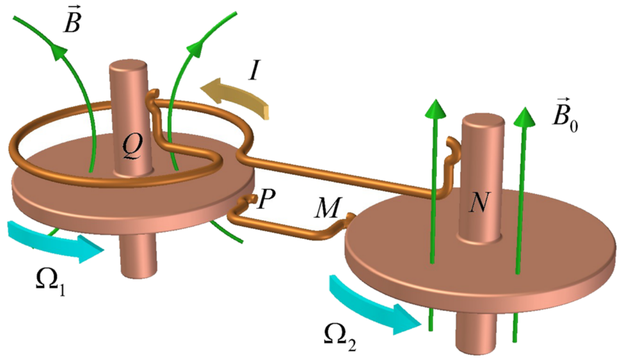

Fig. 2. The current provided by a Bullard dynamo is used to drive a Faraday disk in the external magnetic field B_0.

$$J\frac{d\Omega_2}{dt} = \alpha B_0 I - \lambda\Omega_2. \tag{7}$$

Equation (3) for Ω_1 is unchanged.

We first assume that Ω_1 is constant and perform a linear stability analysis of the solution $I = 0$. We look for solutions proportional to e^{st} for I and Ω_2 and obtain the characteristic polynomial for s from Eqs. (6) and (7),

$$JLs^2 + (\lambda L + JR - JM\Omega_1)s + \lambda(R - M\Omega_1) + (\alpha B_0)^2 = 0. \tag{8}$$

Although the calculation of the roots of this polynomial is straightforward, it is easier to discuss the nature of the bifurcations by considering when the coefficients of the polynomial vanish.

A stationary instability occurs when the constant term in s vanishes, that is, $\Omega_1 = \Omega_{1c} = R/M + (\alpha B_0)^2/\lambda M$, provided that the coefficient of s is positive. This solution requires that $(\alpha B_0)^2 < \lambda^2 L/J$. Thus, when the external magnetic field B_0 is small enough, the nature of the bifurcation of the solution $I = 0$ is unchanged compared to the Bullard dynamo alone. It remains a stationary bifurcation.

If the coefficient of the term proportional to s vanishes first when Ω_1 is increased, we obtain two pure imaginary solutions $s = \pm i\omega_0$ provided that the constant term in s is positive, that is, $(\alpha B_0)^2 > \lambda^2 L/J$. In this case the unstable mode is oscillatory with a pulsation ω_0 and results from a Hopf bifurcation. Thus, for B_0 sufficiently large, I and Ω_2 grow in an oscillatory fashion. The amplitude of this growing oscillation saturates when Eq. (3) is taken into account instead of assuming Ω_1 constant, and the system converges to a limit cycle. We thus find surprising behavior when the current provided by a dynamo drives a similar electric motor[16]—the current and the angular velocity of the motor display periodic reversals.

There is a point in the two-parameter space (Ω_1, B_0) for which the stationary and the oscillatory instability occur concomitantly when both the term proportional to s and the one independent of s simultaneously vanish, that is, when $(\alpha B_0)^2 = \lambda^2 L/J$ and $\Omega_1 = R/M + \lambda L/JM$. This case is called a codimension-two bifurcation point.[2,3] Rich dynamics occur in its vicinity including chaotic regimes if Eq. (3) is also taken into account.

III. DYNAMO EXPERIMENTS USING UNIVERSAL MOTORS

We use two commercial universal motors of the type used in washing machines. These motors contain two coils wounded around the polar pieces of the stator, a ferromagnetic structure. When a current circulates through these coils, a magnetic field is produced in the space between the poles, where a cylindrical ferromagnetic structure can rotate. This component, the armature, contains a set of coils whose terminals are connected to the copper segments of a commutator, which rotates along with the armature. The electrical contact between the coils and the external circuit is made through non-rotating brushes in sliding contact with the commutator. The function of the commutator and brushes is to maintain a nearly constant distribution of currents in the armature with respect to the poles of the stator, no matter the angular position of the armature. A description of this type of motor for non-specialists can be found in Ref. 17.

The armature, or rotor, plays the same role as the disk in the Bullard dynamo, and the stator plays the role of the coil. To make this analogy explicit, we introduce a simplified version of the evolution equation of the motor. An important term is the magnetic flux $\phi(I_s)$ created in the rotor by the stator current, I_s. When the armature rotates at angular velocity Ω, a voltage $\Omega\Phi(I_s)$, with $\Phi(I_s) = K\phi(I_s)$, is generated between the brushes. The constant factor K takes into account the number of turns in the coils and the geometry of the magnetic circuit. For simplicity, we call $\Phi(I_s)$ the magnetic flux.

If an angular speed Ω is imposed to the rotor and a resistor is externally connected between the brushes, the current satisfies

$$L\frac{dI}{dt} = \Omega\Phi(I_s) - RI, \tag{9}$$

where L is the total inductance of the coils, which for simplicity we consider constant, and R is the total resistance of the circuit. If we consider that the current in the rotor is injected in the stator, so that $I_s = I$, and if we assume that Φ is linear in the current, we recover Eq. (2) for the current in the Bullard dynamo.

The mechanical equation for the rotor is

$$J\frac{d\Omega_1}{dt} = \Gamma_a - I\Phi(I_s), \tag{10}$$

where Γ_a is the sum of the friction torque and the externally applied torque. As discussed for the Bullard dynamo, the term $I\Phi(I_s)$ can be obtained using conservation of energy. Equation (10) follows from the fact that the power of the electromotive force $I \times \Omega\Phi(I_s)$ is equal in magnitude to the power of the Lorentz force $-\Omega \times I\Phi(I_s)$.

Some of these quantities are easily measured. The resistance of the rotor is of the order of 5Ω, and the resistance of the stator is approximately 3Ω. The inductance of the rotor is 20 mH and the inductance of the stator is 70 mH. The value of Φ can be experimentally determined by feeding a current I_s to the stator and measuring the rotor open circuit voltage ΔV as a function of Ω. By using $\Delta V = \Omega\Phi\,(I_s)$, we determine Φ (see Fig. 3). A simple model of its complex behavior which neglects hysteresis is

$$\Phi(I) = f_0 \tanh(I/I_0). \tag{11}$$

Although Eq. (11) implies that the inductance L in Eq. (9) is a function of the current, we assume that it is constant, which introduces no qualitative changes in the dynamics. To determine J, we fix the value of I_s and apply a periodic

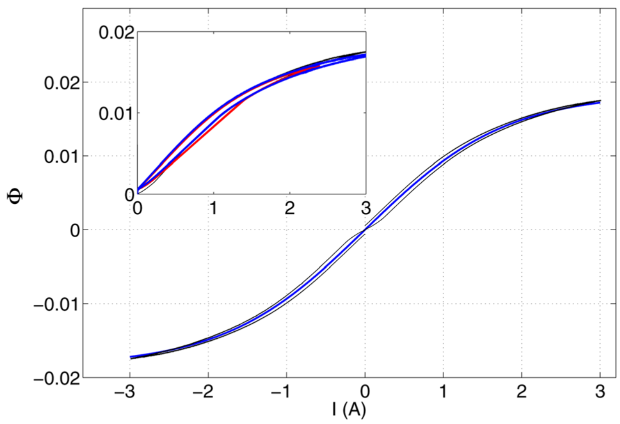

Fig. 3. Magnetic flux Φ measured at the rotor as a function of the current in the stator. The thin line is obtained by applying a fixed current at the stator and measuring the voltage at the rotor. The thick line is the model in Eq. (11) with $I_0 = 1.8$ A and $f_0 = 0.0185$. In the inset, Φ is displayed as a thin line together with the flux (thick lines) obtained from the time series of Fig. 4, assuming a stationary solution for Eq. (9).

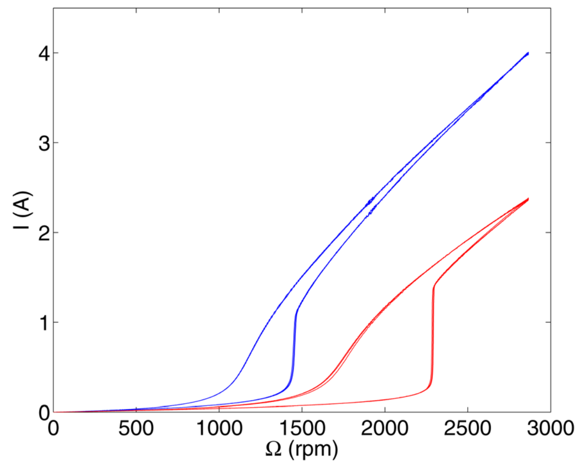

Fig. 4. Current generated in a circuit by a dynamo with resistance $R = 6\Omega$ and $R = 12\Omega$. The angular velocity Ω of the dynamo is increased from 0 to 2900 rpm (lower branch) and then decreased to 0 (upper branch) for a total duration of 300 s. Three cycles are present (almost not discernable).

current I with angular frequency ω to the rotor. By performing measurements at different values of ω, we can calculate J from $J = \Phi(I_s)\sigma(I)/(\sigma(\Omega_1)\omega)$, where $\sigma(I)$ denotes the standard deviation. This procedure gives $J \simeq 1.38 \times 10^{-4}$ kg m^2.

Note that the resistance of the rotor depends strongly on the contact with the brushes. After running the motor for a while, this resistance can be much different from the one measured at the beginning of the experiment. Frequent cleaning of the commutator improves the reproducibility of the measurements.

IV. GENERATION OF ELECTRIC CURRENT FROM THE DYNAMO INSTABILITY OF A MOTOR

A. Dynamo operated at fixed velocity

Given the properties of the motor, we now describe its use as a dynamo. The stator, the rotor, and a load resistance R are connected in series. The rotor is put into motion by another motor. We consider two possible ways to operate the dynamo by either fixing its velocity or the applied torque.

In Fig. 4, we display the evolution of I as a function of Ω when the velocity is controlled and slowly varied from 0 to its maximum value and back. For increasing Ω, we observe a sharp transition from a small current to a larger one. A decrease of Ω smoothly reduces I to small values.

The bifurcation is somewhat surprising. The simple model given by Eqs. (9) and (11) predicts a bifurcation for the critical value $\Omega_c = RI_0/f_0$. The system bifurcates with no hysteresis from $I = 0$ for $\Omega \leq \Omega_c$ to $I \propto \pm\sqrt{\Omega - \Omega_c}$ for $\Omega \geq \Omega_c$. The disagreement between this model and the experimental observations is due to the complicated relation between Φ, I_s, and the history of the system. If we assume a stationary solution of Eq. (9), RI/Ω provides a measure of Φ independent of the one presented in Sec. III (see the inset of Fig. 3). We observe that the flux varies slightly depending on whether Ω is increased or decreased, a feature that traces back to the properties of the ferromagnetic material of which the motor is made.

To understand how the flux affects the bifurcation diagram, we note that the stationary values of the current generated in the dynamo can be determined graphically by the intersection between $\Phi(I)$ and RI/Ω, whose slope varies from $+\infty$ to 0 as Ω increases. The precise shape of Φ is responsible for the form of the bifurcation diagram. For low rotation rates, the existing remanent flux, $\Phi(I_s = 0) > 0$, is responsible for the imperfectness of the bifurcation, that is, the current does not exactly vanish before the startup of the dynamo. As I increases, $\Phi(I)$ has an inflection point: its slope initially increases with I and then decreases due to the saturation of iron. This behavior implies that $\Phi(I) = \lambda I$ may have more than one solution. For a certain value of λ, that is, of R/Ω, two solutions are equal and disappear for larger Ω. This change in the number of solutions results from a saddle-node bifurcation which is responsible for the discontinuous increase of I when the dynamo starts.

The flux for decreasing values of I is a convex positive function. Therefore only one solution of $\Phi(I) = \lambda I$ exists, and its value decreases continuously as Ω decreases. The bifurcation can be described as an imperfect pitchfork with $I \propto \pm\sqrt{\Omega - \Omega_c}$ for $\Omega \geq \Omega_c$. For decreasing Ω, I connects with the branch corresponding to a small value due to the remanent magnetization.

B. Dynamo operated at fixed torque

The dynamo can also be operated by controlling the applied torque Γ_a. We apply a ramp of increasing torque followed by a ramp of decreasing torque and show the bifurcation diagram as a function of Γ_a in Fig. 5. We see that the transition is continuous and displays the scaling of a usual pitchfork bifurcation.

In Fig. 6, we display the different terms involved in Eq. (10). For a small applied torque, the torque of the Lorentz force $I\Phi(I)$ vanishes and the torque of the applied force is balanced by friction and the inertia of the rotor. Once the dynamo starts and for Γ_a larger than a critical torque $\Gamma_{a,c}$, the torque of the Lorentz force increases and roughly balances the excess of torque $\Gamma_a - \Gamma_{a,c}$.

The nature of the bifurcation depends on whether Ω or Γ_a is the control parameter. To explain this difference, consider the asymptotic expression of the flux: $\Phi \simeq \Phi_0(I + aI^3)$ with $a > 0$, which is applicable for small I if the flux is not convex. If Ω is the control parameter, the stationary solutions are $I = 0$ or $\Omega = RI/\Phi(I) \simeq R(1 - aI^2)/\Phi_0$. If we let

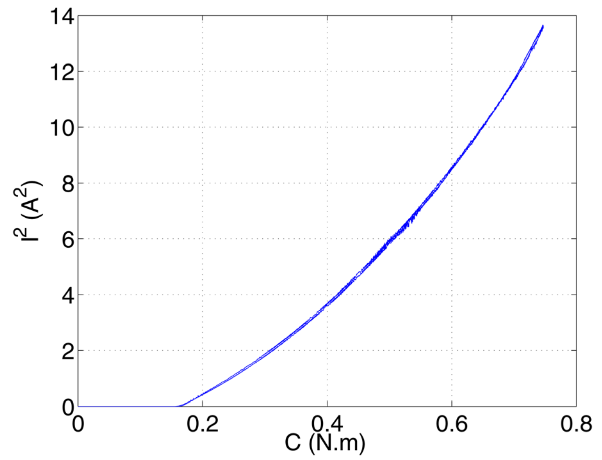

Fig. 5. Square of the current as a function of applied torque. The scaling of a usual pitchfork bifurcation is recovered, that is, $I^2 \propto \Gamma_a - \Gamma_{a,c}$ close to threshold.

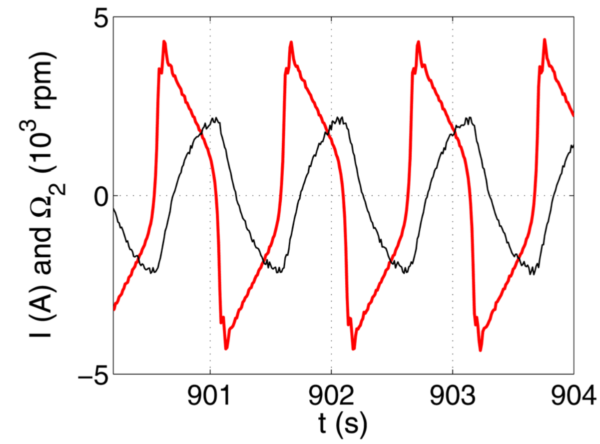

Fig. 7. Time series of the current I (thick) and the angular velocity Ω_2 (thin) of the motor in the oscillatory regime for $I_s = 0.7$ A and Ω_1 slightly above the threshold of the oscillatory regime.

$\Omega_c = R\Phi_0$, we obtain the pair of solutions $I^2 = -(\Omega - \Omega_c)/(a\Omega_c)$. These solutions exist for $\Omega < \Omega_c$ which indicates that the bifurcation is subcritical.

If we assume that Γ_a is the control parameter and assume, for simplicity, that the fluid friction term $\lambda\Omega$ slows down the rotor, the stationary solutions satisfy $\Gamma_a = \lambda\Omega + I\Phi(I)$ and $\Omega\Phi(I) = RI$. Thus $\Gamma_a = I[(\lambda R/\Phi) + \Phi] \simeq \lambda R/\Phi_0 + I^2(1 - a\lambda R/\Phi_0)$. If the coefficient of I^2 is positive, the bifurcation is supercritical. We denote the critical torque by $\Gamma_{a,c} = \lambda R/\Phi_0$ and obtain $I \propto \pm\sqrt{\Gamma_a - \Gamma_{a,c}}$. The bifurcation diagram of this dynamo shows that the nature of a bifurcation (supercritical versus subcritical) depends on the choice of control parameter.

The stator is subject to a frictional torque which involves both solid and fluid components. By applying a fixed torque to the rotor, it is possible to estimate the significance of these effects. For the motors we used, these quantities depend on several parameters, including the mechanical contact at the brushes and may change during the experiment. For the simplified low-dimensional models that we will introduce in what follows, we assume that the applied torque compensates for the solid friction term, and we will not model the effects of the difference between static and dynamic frictions.

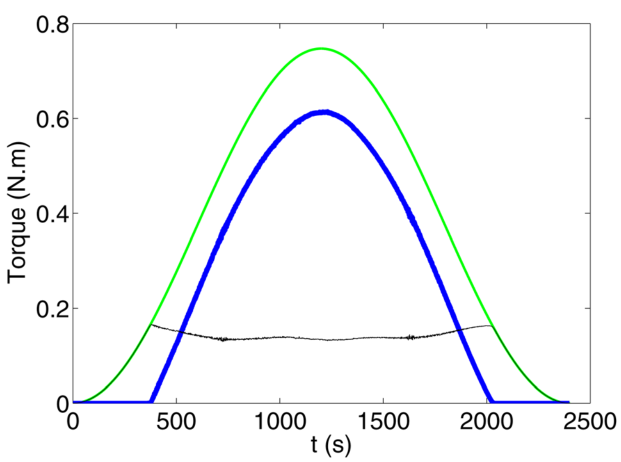

Fig. 6. Time series of the applied torque Γ_a (medium), the torque of the Lorentz force $I\Phi(I)$ (thick), and the difference between them $\Gamma_a - I\Phi(I)$ (thin). The units of the torque are in N m. A varying torque is applied. Once the dynamo is on, the excess of torque is balanced by the torque of the Lorentz force.

V. DYNAMICAL REGIMES OF A DYNAMO DRIVING A MOTOR

A. Fixed velocity: A codimension-two bifurcation

We now consider a motor which works as a dynamo and is connected in series with a second motor. In the latter, the stator current I_s is fixed and has no electrical contact with the rotor. When the dynamo is on, it generates a current which circulates in the rotor of the motor and puts it into motion.

We fixed the stator current I_s and varied the angular velocity Ω_1 of the dynamo. For low I_s and large values of Ω_1 a stationary regime is observed: the dynamo generates a current I and the motor rotates at angular frequency Ω_2 with I and Ω_2 nearly constant. When I_s is large, we observe a different regime. For large Ω_1, the system oscillates. In Fig. 7, we display time series of the dynamo current and the motor angular velocity Ω_2. The two signals are out of phase: a positive current accelerates Ω_2 and a large Ω_2 reduces I. These opposite effects are the cause of the observed oscillation.

The simplified equations for the evolution of the system in which these two effects appear in the terms proportional to $\Phi(I_s)$ are

$$L\frac{dI}{dt} = \Omega_1\Phi(I) - RI - \Omega_2\Phi(I_s), \qquad (12)$$

$$J\frac{d\Omega_2}{dt} = I\Phi(I_s) - \lambda\Omega_2. \qquad (13)$$

We recover the equations discussed in Sec. II if Φ is assumed to be linear in I. The period of oscillation T_0 slightly above threshold is displayed in Fig. 8. Its behavior is of the form $T_0^{-2} \propto I_s - I_{sc}$, where I_{sc} is the critical current above which the oscillation is observed, its pulsation being given by the imaginary part of the solution of Eq. (8).

We note that as for a single dynamo, the bifurcation depends on how the experiment is performed. In particular, the values of the thresholds depend on whether Ω_1 is decreased or increased.

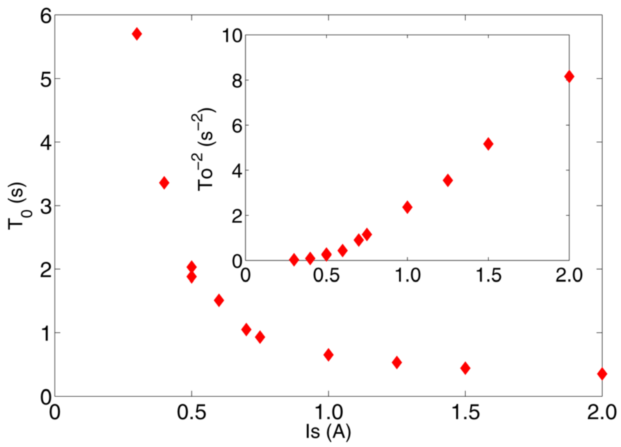

Fig. 8. Period T_0 of the current at the onset of the oscillatory regime as a function of the stator current I_s. T_0^{-2} is displayed in the inset.

B. Fixed torque: Chaotic regimes

When the system is operated at fixed dynamo velocity, it is described by two degrees of freedom, I and Ω_2, so that the phase space is two-dimensional. In this case dynamical systems theory states that stationary or oscillatory solutions are the generic behaviors,[3] and no low-dimensional chaos is expected. The situation is different when the dynamo is operated at fixed torque. The angular velocity becomes an additional degree of freedom and phase space is now three-dimensional.

The parameter space, displayed in Fig. 9 is very rich. A transition to a regime of a time-independent dynamo is observed for low torque. If I_s is sufficiently large, an increase of the torque results in transitions which generate a variety of regimes: chaotic reversals, nearly harmonic oscillations, and strongly anharmonic ones.

Examples of time series are presented in Fig. 10. In Fig. 10(a) the current displays strongly anharmonic oscillations and reaches large values before approaching a quasi-stationary phase. During the phases in which the current is

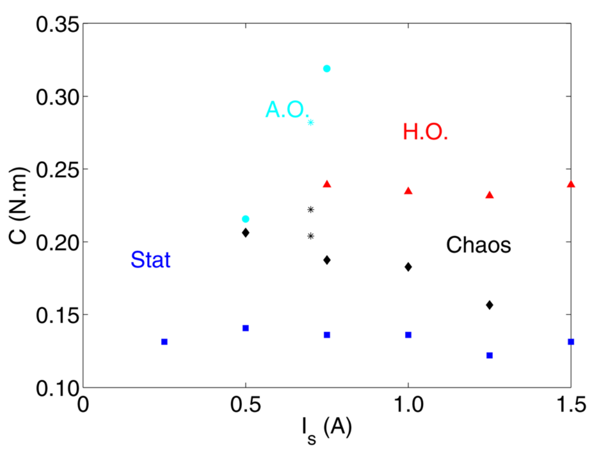

Fig. 9. Parameter space for a dynamo connected to a motor. A fixed current I_s is injected in the stator of the motor. Measurements are performed while increasing torque Γ_a is applied to the dynamo. A stationary current is generated above a critical torque (squares). For large enough I_s, a subsequent increase of the torque (diamonds) results in a regime of chaotic reversals of the current. Further increase of the torque leads to anharmonic oscillations (open circles) or nearly harmonic ones (triangles). The stars correspond to the time series displayed in Fig. 10.

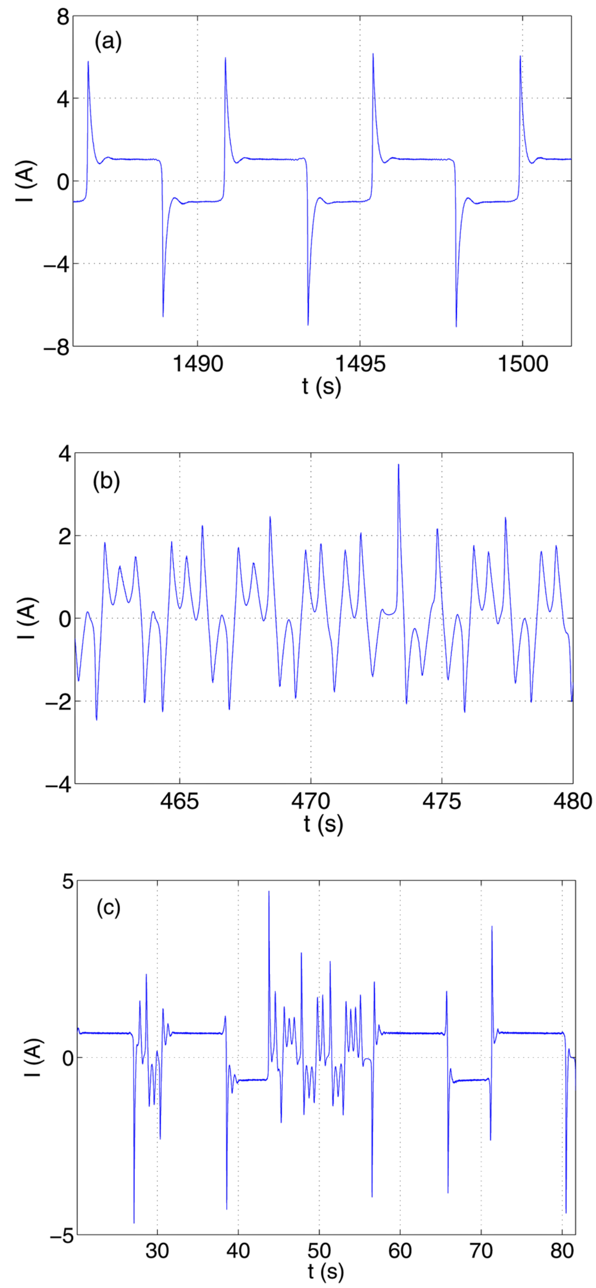

Fig. 10. Time series of the current I of the dynamo in a regime of anharmonic oscillations for (a) $I_s = 0.7$ A and $\Gamma_a = 0.28$ N m, in chaotic regimes of random reversals, with (b) $I_s = 0.7$ A and $\Gamma_a = 0.22$ N m, and (c) $I_s = 0.7$ A and $\Gamma_a = 0.20$ N m.

nearly constant, the angular velocities Ω_1 and Ω_2 increase until the current suddenly changes sign. Other oscillatory regimes are observed (not displayed) in which the current I does not display these stationary phases. These time series, which are qualitatively similar to the one displayed in Fig. 7, are termed nearly harmonic oscillations in contrast to the strongly anharmonic ones. In Fig. 10(b) the system displays random behavior. The current oscillates one, two, or three times around a nonzero mean value and then reverses toward the opposite value around which it starts to oscillate. This behavior is reminiscent of solutions of the Lorenz equations in the regime where chaotic trajectories connect domains in phase space in which a stationary state is unstable with complex conjugate eigenvalues. In other words, the system

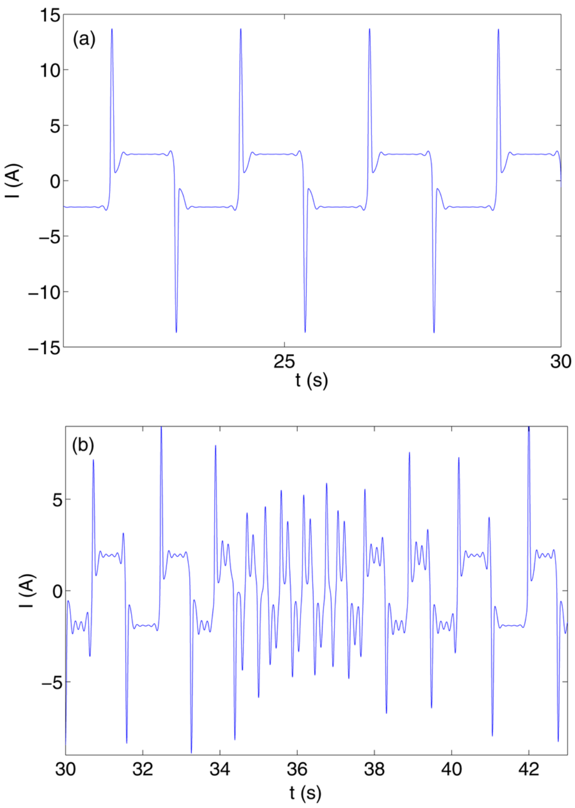

Fig. 11. Time series of the solutions of Eqs. (12)–(14). The time series are similar to the series in Figs. 10(a) and 10(c).

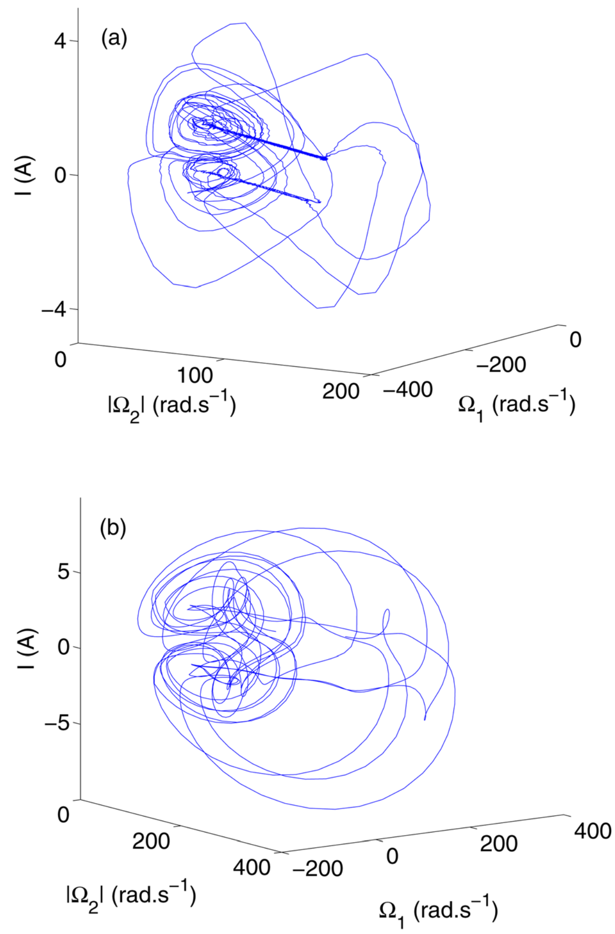

Fig. 12. Phase space (I, Ω_1, and $|\Omega_2|$) for (a) the experimental time series displayed in Fig. 10(c); and for (b) the numerically computed time series displayed in Fig. 11(b).

displays growing oscillations in a neighborhood of an unstable solution. When the amplitude is large, the trajectory evolves toward a neighborhood of the opposite unstable solution and resumes oscillating. Another regime is presented in Fig. 10(c). The system displays phases of roughly constant current $\pm I_c$ and switches randomly between these states. All these regimes can be obtained from the numerical solutions of Eqs. (11)–(13), supplemented by a mechanical equation for the rotor of the dynamo

$$J\frac{d\Omega_1}{dt} = \Gamma_a - I\phi(I). \tag{14}$$

Computed time series in the regimes of anharmonic oscillations and random reversals are displayed in Fig. 11. The structure of phase space is revealed in Fig. 12 where trajectories are shown from the experiment and the numerically computed time series. The phase space helps to understand the origin of the chaos in the experiment. Trajectories approach $\pm I_c$ following a spiral ($\pm I_c$ has two attractive directions with complex conjugate eigenvalues). These trajectories are repelled in a third direction (with a positive eigenvalue). This phase space behavior in the vicinity of a fixed point is well known to generate chaos, following the Shilnikov scenario.[3]

The experimental set-up is more sophisticated than the set of equations. The latter does not take into account the (possibly complicated) solid friction terms, the hysteric dependence of Φ on the current I, and the decrease of the inductance L at large currents due to saturation of the ferromagnetic material. These effects are not necessary to generate the complex chaotic behavior of the system. However, it might be necessary to take them into account to make a more quantitative comparison between experiment and the low dimensional model.

VI. CONCLUSION

We have presented a set of experiments using low cost universal motors in which a variety of bifurcations can be observed and several properties can be measured quantitatively. The experiments can be used in a laboratory course or be presented as introductory illustrations in courses on bifurcation theory or dynamical systems. In addition, when a dynamo is operated at fixed torque and drives a motor, chaotic regimes are observed, including random reversals of the current and of the rotation of the motor.

Several other experiments can be performed. When two dynamos are connected in parallel with a resistance, saddle-node bifurcations can be observed between a regime in which the two dynamos inject a current in the resistance and a regime where the two dynamos generate opposite currents and no current flows in the resistance. When two dynamos are used such that the stator of one of the dynamos is connected to the rotor of the second one (and vice versa), time dependent regimes, including regimes of random reversals, are expected to be observed. This set-up is similar to the Rikitake dynamo.[18]

Recently, dynamical regimes of the magnetic field generated by a dynamo process due to a swirling flow of liquid sodium have been observed.[19,20] Despite the large intensity of turbulent velocity fluctuations (the kinetic Reynolds number is larger than 10^6), the dynamics of the large scale magnetic field remains low dimensional and involves two modes. In the vicinity of their thresholds, the equations for the amplitude of the modes are constrained by the symmetries of the system[21] and, to leading order, are of the form of Eqs. (6) and (7). In the fluid dynamo experiment, effect of the turbulent fluctuations is important in the vicinity of some instability thresholds. In particular, they initiate random reversals when the system is close to a saddle-node bifurcation. In contrast, in the system presented here the source of randomness is associated with the presence of a third mode (the dynamo angular velocity) which is coupled to the dynamo current and to the rotation rate of the motor.

We conclude by pointing out that the experiments we have discussed are an original approach to the rich behavior of coupled electromechanical devices. They illustrate some aspects of the problems of conversion and transport of energy, which are old topics but are likely to regain importance in the future.

ACKNOWLEDGMENTS

R.L. is indebted to G. Bobadilla, S. Navarro and G. Palma, whose support made possible his participation in this work in the frame of a sabbatical year project.

[1] G. Iooss and D. D. Joseph, *Elementary Stability and Bifurcation Theory* (Springer, Berlin, 1980).
[2] V. Arnold, *Geometrical Methods in the Theory of Ordinary Differential Equations* (Springer, Berlin, 1982).
[3] J. Guckenheimer and P. Holmes, *Nonlinear Oscillations, Dynamical Systems and Bifurcations of Vector Fields* (Springer, Berlin, 1983).
[4] P. G. Drazin, *Nonlinear Systems* (Cambridge U.P., Cambridge, 1992).
[5] A. B. Pippard, *Response and Stability* (Cambridge U.P., Cambridge, 1985).
[6] M. I. Rabinovich and D. I. Trubetskov, *Oscillations and Waves in Linear and Nonlinear Systems* (Kluwer Academic Press, Dordrecht, 1989).
[7] A. A. Andronov, A. A. Vitt, and S. E. Khaikin, *Theory of Oscillations* (Pergamon, Oxford, 1966).
[8] G. Nicolis and I. Prigogine, *Self-Organization in Nonequilibrium Systems* (John Wiley & Sons, New York, 1977).
[9] S. Chandrasekhar, *Hydrodynamic and Hydromagnetic Stability* (Oxford U.P., Oxford, 1961).
[10] R. J. Stephenson, "Experiment with a unipolar generator and motor," Am. J. Phys. **5**, 108–110 (1937).
[11] G. Baker and G. Bradley, "A small scale dc motor experiment for the elementary laboratory," Am. J. Phys. **21**, 689–690 (1953).
[12] S. Bednarek, "Unipolar motors and their application to the demonstration of magnetic field properties," Am. J. Phys. **70**, 455–461 (2002).
[13] Y. Kraftmakher, "Experiments with a dc motor," Eur. J. Phys. **31**, 863–870 (2010).
[14] P.-H. Ng, S.-L. Wong, and S.-Y. Mak, "Efficiency measurement using a motor-dynamo module," Phys. Educ. **44**, 639–643 (2010).
[15] C. W. Siemens, "On the conversion of dynamical into electrical force without the aid of permanent magnetism," Proc. R. Soc. London **15**, 367–369 (1866–1867).
[16] M. A. Witz, "Recherches sur les inversions de polarité des série-dynamos," J. Phys. Theor. Appl. **8**, 581–586 (1889).
[17] A. Hugues, *Electric Motors and Drives. Fundamentals, Types and Applications*, 3rd ed. (Newnes, Oxford, 2006).
[18] T. Rikitake, "Oscillations of a system of disk dynamos," Proc. Cambridge Philos. Soc. **54**, 89–105 (1958).
[19] M. Berhanu *et al.*, "Magnetic field reversals in an experimental turbulent dynamo," Eur. Phys. Lett. **77**, 59001-1–5 (2007).
[20] F. Ravelet *et al.*, "Chaotic dynamos generated by a turbulent flow of liquid sodium," Phys. Rev. Lett. **101**, 074502-1–4 (2008).
[21] F. Pétrélis and S. Fauve, "Chaotic dynamics of the magnetic field generated by dynamo action in a turbulent flow," J. Phys. Condens. Matter **20**(49), 494203-1–6 (2008); F. Pétrélis *et al.*, "Simple mechanism for reversals of Earth's magnetic field," Phys. Rev. Lett. **102**(14), 144503-1–4 (2009).

Information on a supplemental simulation for this article appears on the next page.

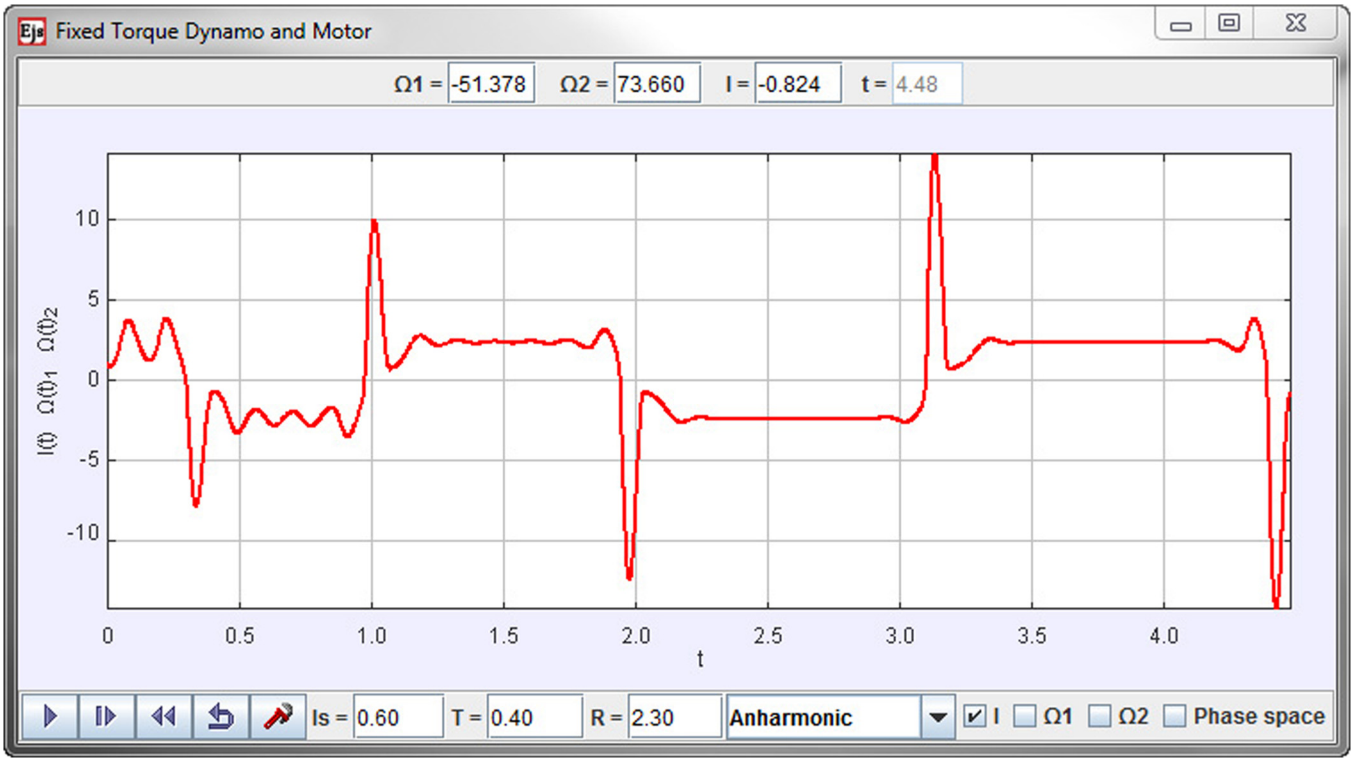

The Fixed Torque Dynamo and Motor Model solves the coupled differential equations for an electric motor driven by a dynamo (generator). The model can be used to illustrate elementary instabilities or bifurcations discussed in courses on nonlinear oscillators and dynamical systems. When the dynamo is driven at constant torque, chaotic reversals of the generated current and of the angular rotation of the motor are observed. The main window displays the dynamo angular velocity (Ω1), motor angular velocity (Ω2), and current (I) time series, while a second window displays the phase space. The stator current (Is), torque (T), and resistance (R) are adjustable.

http://www.compadre.org/osp/items/detail.cfm?ID=11528

A 3D Faraday Disk Dynamo Model by Anne Cox that shows a conducting disk rotating in a magnetic field is also available.

http://www.compadre.org/osp/items/detail.cfm?ID=9417

The Fixed Torque Dynamo and Motor Model is a supplemental simulation for the paper by C. Laroche, R. Labbé, F. Pétrélis and S. Fauve, and has been approved by the authors and the AJP editor. Partial funding for the development of these models was obtained through NSF grant DUE-0937731.

Wolfgang Christian